Process Physics and Modeling in Semiconductor Technology, ed. J. D. Plummer, S. T. Pantelides and G. R. Srinivasan, Vol. 91, 3 (1991).

# MOLECULAR DYNAMICS SIMULATIONS OF GROWTH AND ETCHING REACTIONS ON SILICON SURFACES

*D. Srivastava, T. A. Schoolcraft and B. J. Garrison*
Department of Chemistry
The Pennsylvania State University
University Park, PA 16802

## Abstract

Molecular dynamics (MD) simulations are employed to study molecular-beam epitaxy (MBE) of Si and Ge thin films on the (2x1) dimer reconstructed surface of Si{100} and F atom reaction with the same surface. In MBE growth on Si{100}-(2x1) surface the deposited atoms must not only spread out smoothly to achieve layer by layer growth, but the surface dimers must open to allow the epitaxial growth. We have observed in the calculations mechanisms of dimer openings that lead to epitaxial growth. The results reveal a novel mechanism of collective dimer openings in which diffusing adatoms move perpendicular to the direction of the dimer rows on the original surface. The resulting relaxation of the dimer atoms and the underneath substrate causes the opening of successive dimers along the way. This is in agreement with recent scanning tunneling microscope (STM) studies which show that the epitaxial layer grow preferentially in a direction perpendicular to the original dimer rows on the surface. The etching of silicon proceeds facilely by the addition of F atoms to the surface. The sticking probability of near thermal fluorine atoms on the reconstructed Si{100}-(2x1) surface as a function of F coverage is calculated. The sticking probability on the clean Si surface is not unity, and it decreases to approximately zero for fully fluorinated surface. The results agree qualitatively with the experiments, and also closely follow the Langmuir adsorption curve. When the surface is half fluorinated the sticking probability deviates from those of the Langmuir values for certain assumed geometries. The role of surface diffusion and channeling in causing these deviations is explored.

## *I. Introduction*

The study of the growth and etching reactions of semiconductors is important in understanding and fabricating microelectronic devices with the desired electronic behavior. Efforts on both the theoretical and experimental fronts are pursued to understand atomic level details of these reactions. Molecular-beam epitaxy (MBE) is one of the most widely employed techniques for growing semiconductor thin films. In this method, atoms or molecules effuse from an oven source of semiconductor material and impinge on a constant temperature semiconductor substrate. The layers of deposited material often form high quality, defect free, single crystal thin films. Depending upon growth conditions the film could have the same well defined crystalline structure of the underlying substrate (epitaxial) or it could have entirely different bonding structures (amorphous). The usual goal is to obtain layer by layer epitaxial growth so that alternating bands of different semiconductor materials can be grown to form superlattices of the desired electronic properties (1). One of the problems with obtaining layer-by-layer growth is the fact that atoms in the surface layer of most semiconductors are significantly displaced from the bulk configuration. For example, the surface atoms on the bulk terminated Si{100} face [Fig. 1a] tend to move closer to the neighboring atoms and form rows of stable dimer structures [Fig. 1b]. These structures have been confirmed both through theoretical energetics calculations (2) and through direct scanning tunneling microscope (STM) (3,4) studies. In order for epitaxial growth to occur on a reconstructed surface [Fig. 1b], the atoms in the dimerized layer must be reordered back to their original bulk positions, and the atoms in the deposited layer must find themselves in the expected bulk positions for the next higher layer. A number of experimental advances in recent years allows one to observe the growth characteristics on a microscopic level (3-5). The problem from our point of view is that these observations are made seconds to minutes (an infinite amount of time) after the interesting chemical reactions of dimer opening or surface rearrangements have occurred. It is mainly in this time regime the molecular dynamics computer simulations can be useful in studying the atomic level details of the dimer opening reaction on the substrate surface layer and the epitaxial formations in the deposited layers.

The etching of silicon is done in the presence of a plasma in which fluorine atoms are the dominant species. Fluorine reacts with the substrate silicon atoms to form volatile species such as silicon tetrafluoride, $SiF_4$, thus transferring one silicon atom from the solid substrate to the gas phase. Due to the difficulties involved in making atomic fluorine beams, however, only a few experiments (6,7) have explored the details of fluorine atom reaction with crystalline silicon. Even though, the final etch product observed in these experiments is mainly the gaseous $SiF_4$, a 15-20Å thick intermediate surface region consisting of one to three F atoms bonded to Si atoms has also been reported (8). Again molecular dynamics simulations can be useful (9,10) in studying mechanisms of a gas phase F atom reaction with Si solid.

Recently using Tersoff's many-body potential for the multicomponent Si-Ge systems (11) and Stillinger-Weber's potential for Si-F interactions (12), we have reported MD simulations of the MBE growth of Si and Ge thin films on Si{100}-(2x1) surface (13,14) and the reaction of crystalline silicon with gas phase F atoms (15), respectively. The individual and collective surface dimer openings on the substrate surface leading to the formation of (2-4 layers thick) epitaxial region in the deposited layers were observed in these simulations (13,14). Atomistic details of the dimer opening reaction sequence revealed a novel mechanism of the collective motion of adatoms (deposited atoms) in which the diffusing adatoms move perpendicularly to the direction of dimer rows in the underneath layer and open successive dimers (13). The reaction implied a dramatic enhancement of crystal growth in the direction perpendicular to the direction of the dimer rows on the original reconstructed surface. Concurrently with these predictions, the same anisotropy in the early stages of the epitaxial growth was also discovered in STM studies (16,17). In the simulation of F atom adsorption on Si{100}-(2x1) surface (15), it was noted that the sticking probability of near thermal F atom on clean surface is close to unity. As the coverage of fluorine on the surface increases the sticking probability decreases. On a fully fluorinated Si surface the sticking probability increases once the ion kinetic energy of the incoming atom is increased to more than 0.5 eV. In this work, we describe details of the microscopic reactions that occur on the reconstructed Si{100}-(2x1) surface when it interacts with near thermal Si, Ge and F atoms. The emphasis in the first two cases is on the dimer opening reactions in the initial stages of the epitaxial growth, and in the third on the sticking as a function of the fluorine coverage. In section II, we describe the growth and adsorption reaction simulation systems and the interaction potentials employed in this study. Section III deals with microscopic reactions in the initial stages of the epitaxial growth of Si and Ge thin films on Si{100}-(2x1) surface, readers are referred to elsewhere for the macroscopic growth characteristics (14). In section IV we describe F atom sticking on Si{100}-(2x1) surface as a function of coverage, and lastly in section V we summarize the results of this work.

## *II. Simulations of the Growth and Etching Reactions on Si{100}-(2x1) Surface*

In molecular dynamics simulations of the MBE growth of semiconductors the gas phase atoms of the semiconductor material are randomly deposited on a constant temperature substrate slab. The non-equilibrium dynamics of the substrate and the deposited atoms, interacting with realistic many-body forces, is evolved by solving classical equations of motions in finite short time steps ($\sim 10^{-15}$ seconds) for long time ($\sim 10^{-9}$-$10^{-8}$ seconds) durations. Our molecular dynamics simulation consists of maintaining 10 layers with 32 atoms/layer in the slab. The atoms in the bottommost layer are anchored in position with the atoms in the next four layers forming a stochastic region. The atoms in the top five layers and all the deposited atoms are considered "real atoms" and move only under the influence of the interaction potential. The atoms in the stochastic region experience the forces due to the interaction potential and a frictional force. The magnitude of the friction force is

proportional to the temperature of the system (19). As the temperature of the system rises (falls) due to physical or chemical interaction between the substrate and the deposited atoms, the magnitude of the frictional forces on the atoms in the stochastic region is increased (decreased) proportionally to damp high (low) temperature oscillations of these atoms. The stochastic region, therefore, facilitates the flow of kinetic energy into and out of the system and maintains a constant temperature. The separation of the full system into an interaction region (top five layers) and a stochastic region (bottom four layers) makes dissipation of excess energy into the stochastic region rather slow, but the dynamics in the interaction region is more accurate and is a better representative of the true dynamical behavior of the interaction potential. The top surface layer [Fig 1b.] initially consists of 16 dimers which are arranged in rows. Periodic boundary conditions which simulate an infinite surface were employed along the surface plane. The structure with neatly arranged rows of dimers has been used in previous simulations of epitaxial growth (13,14), and has also been observed in direct STM studies (3,4). The deposition rate of Si and Ge atoms at 1 atom/2-3 ps (1 ps = $10^{-12}$ second) is sufficiently slow so as to allow equilibration of the system before the arrival of the next atom. It has been pointed out in an earlier study (20) that if the deposition rate is too fast to allow for complete dissipation of the kinetic energy from the exothermic adsorption reactions, then the excess energy in the interaction region effectively destroys the structure of the interface of the originally reconstructed surface and the layers of the deposited material. The effect of long-time equilibration after the deposition, in that case, is like the simulation of crystallization from a liquid state. After each deposition of 1.5 monolayers of atoms the full system was equilibrated for 0.5 to 1 ns. The dynamic behavior of the deposited and the substrate atoms revealed microscopic and macroscopic features of the growing film.

The interaction potential used in these simulations is Tersoff's many-body potential for Si and Ge (11). In a previous study of the MBE growth of Si/Si{100} system, we have used this potential and have found that for the dimer reconstructed {100} surface it not only gives reasonable energetics of the dimer reconstruction (1.45 eV/dimer) but is also suitable for the simulations of the epitaxial growth. It is noted that in Tersoff's potential the heteroatomic interaction between Si and Ge atoms is introduced simply by a single additional parameter. The rest of all the other parameters are either the arithmetic or the geometric means of the parameters for the isolated Si and Ge atoms, and the functional form of the potential for a multicomponent system remains the same as that of the previous single component case.

The simulation for F atom reaction with Si{100}-(2x1) surface is similar to the method described above for the growth reactions. The Si{100}(2x1) surface is modeled with a microcrystallite of six layers with eight atoms per layer. The top layer is reconstructed into four surface dimers (see Fig. 1a of ref. 15). Each atom in the surface dimers has one dangling bond site that is ripe for fluorine atom attachment. The forces on the atoms in the top two layers were determined from the interaction potential. The next three layers are treated as the stochastic region. The energy function used is a many-body potential developed by Stillinger and Weber

(12). The initial conditions for an F atom deposition are a random vibrational phase in the crystal, a random aiming point on the surface, and a gas phase fluorine atom traveling perpendicular to the surface with a fixed kinetic energy.

A trajectory is considered to be completed when one of three possible results is observed. One result is for the incoming fluorine atom to adsorb on the surface. An atom was counted as adsorbed when its binding energy to the solid is greater than 5.0eV. Another result for the incoming fluorine atom is to be repelled by the surface. The criterion for this event is that the potential energy of the incoming fluorine atom with respect to the surface is zero and its velocity vector is directed away from the surface. The last possible result is for the time of the trajectory to have passed three picoseconds (~10,000 integration steps). This event is not observed for the clean surface, but is occasionally found when the incoming fluorine atom comes within range of a fluorine adatom. Whether this event is an artifact of the potential energy functions or is a realistic description is not known. Any fluorine atom that is diffusing at the end of the trajectory is counted as if it had left the influence of the surface. We believe this approximation to have very little effect on our results. The sticking probability (S) therefore is calculated as the number of favorable events divided by the total number of trajectories. Other details of this calculation are published elsewhere (15).

## *III. Microscopic* reaction *mechanisms of the initial stages of the epitaxial growth.*

A comprehensive picture of the initiation of growth of thin epitaxial films on the Si{100}-(2x1) reconstructed surface can be partitioned into three stages. First there are the atomic level details of the individual dimer openings (an essential step for the initiation of the epitaxial growth). Second there is an intermediate stage where the initially deposited adatoms begin to resemble the first epitaxial layer. Finally the macroscopic growth modes appear where some systematics of the layer by layer growth process can be established and compared with experimental observations. In this work our emphasis is on the microscopic mechanisms of individual and collective surface dimer openings. The effect of the latter is to introduce an anisotropy in the epitaxial growth which is directly observable in laboratory experiments such as STM (16,17). Macroscopic growth modes for depositing a few layers of Si and Ge on the Si{100}-(2x1) surface and the comparison of our predictions with other experimental observations are described in detail elsewhere (14).

### *A. Reaction mechanisms of individual dimer openings.*

The microscopic reaction mechanisms of stable dimer openings (those dimers that remain open for the entire duration of simulation) are basically of two types. First is the diffusing adatom induced mechanism, the typical examples of which are shown in Figures [2a,b]. The Si and Ge adatoms move as shown by the arrows in Figure 2a during the equilibration period (0.5-1.0 ns). First, both the dangling bonds of an isolated dimer are saturated with two adatoms. A third adatom

diffuses over a period of hundreds of picoseconds, to move closer to the dimer, and pushes the adatom on the dangling bond into the epitaxial position. The diffusing adatom itself then occupies the vacant dangling bond of the open dimer. The three adatoms finally occupy the epitaxial positions, whereas the dimer atoms have relaxed back to their bulk positions. Another observed mechanism of the diffusing adatom induced dimer opening is shown in Figure 2b. Instead of pushing the adatom on the dangling bond into the epitaxial position the diffusing adatom can move underneath the adatom on the dangling bond and push the dimer atom into the epitaxial position. In this case, the diffusing adatom has moved into the top substrate layer whereas the substrate dimer atom has moved up into the epitaxial layer. The end products in the homoepitaxy of Si/Si or Ge/Ge, as shown in Figures 2a and 2b are the same. However, in case of the heteroepitaxy of Ge/Si this will cause the formation of a defect at the interface. This defect is formed during the growth event and is not due to interlayer diffusion during an annealing process. In other words, the final configuration in Figure 2a does not convert to the one in Figure 2b during substrate heating.

In the second distinct mechanism of surface dimer openings the atoms in a surface dimer are constantly in motion about their equilibrium positions with amplitudes determined by the temperature of the substrate. During these motions the surface dimers would spontaneously open sufficiently far from their equilibrium separation so that an incoming adatom is directly inserted into the available epitaxial position and thus stabilizes the opening. As shown in Figures 3a-d, we found that the direct insertion of the adatom into epitaxial positions can occur on a bare dimer, on a dimer with one dangling bond occupied, and also on a dimer with both of its dangling bonds occupied. Most of these direct insertion mechanisms occurred during the deposition process, i.e., the surface was relatively clean. The number of such occurrences increased with an increase in the temperature of the substrate. Above room temperature (800~1200K) and during the equilibration period, it was also noted that occasionally a spontaneously opened bare dimer on a relatively clean surface would remain open for hundreds of picoseconds until being stabilized by the direct insertion mechanism. At higher temperatures (1200K as compared to 800K for the Tersoff Si potential) the direct insertion mechanism was the primary reaction mechanism of surface unreconstructions.

In a similar study (21) of the epitaxial growth using a different interaction potential (22), the diffusing adatom motion mechanism was the main mechanism of stable dimer openings, but the total number of such observed openings during 0.5 ns equilibration period was comparatively smaller. In the same study some unstable open dimers due to the insertion of two or more adatoms were also observed. These unstable openings and the resultant structures are not observed in the present simulations. We believe that the higher surface stabilization energy of that potential (22) (2.1 eV/dimer) vs (1.45 eV/dimer) for the Tersoff's potential (11) and the shorter equilibration times of that simulation may have caused the observed differences.

*B. Correlated adatom motion induced anisotropic spread of surface unreconstructions.*

We now discuss a *novel* anisotropic spread of surface dimer openings in the direction perpendicular to the dimer rows on the original reconstructed surface (13). This correlated reaction mechanism dramatically enhances the crystal growth process in one direction as confirmed in recent STM studies (16-17). Details of this correlated adatom motion induced dimer openings are exhibited in Figure [4a-b]. In Figure 4a we show the result of depositing 1.5 monolayers (ML) of Si atoms on the surface over a time span of 144 ps. About half of the deposited atoms are on the dangling bond sites. The remaining atoms are either at the level of the second deposited layer (shown hatched) or form a random overlayer at the level of first deposited layer. During the deposition process four of the original surface dimers were found to open. Two of the openings were due to the direct insertion mechanism, Figure (3), and the remaining two were due a diffusing adatom induced mechanism Figure (2). In one of these later cases the adatom actually replaced one of the original dimer atoms. (Fig. 2b).

The curly arrows in Figure 4a indicate the atomic motion that occurs in the next 512 ps of equilibration at 800K. At this later time the majority of the original surface dimers have opened (Fig. 4b). One sequence of relevant motion starts in the direction of the straight arrow at the bottom of crystal shown in Figure 4a. The adatoms move in the direction of the arrows with dimers opening along the way. Due to the presence of periodic boundary conditions the continuation of the motion (follow the straight arrows) proceeds to the upper left part of Figure 4a. This string of open dimers is perpendicular to the original dimer rows (Fig. 1b). The correlated motion of adatoms inducing a dimer opening does not appear to be dependent on the periodic boundary conditions. This can be seen in another set of correlated motions, which initiate at the lower left corner of the surface in Figure 4a and is terminated only when an amorphous region is encountered as is shown in the upper right corner of the figure. An isolated picture of this later case is shown in Figures 4c. Initially the adatoms are bonded to dimer atoms at the dangling bond positions. This mechanism is a repetition of the mechanism shown in Figure 2a. A cooperative or correlated motion occurs in which the atoms move perpendicularly to the original dimer rows. The final configuration is shown on the right side of the picture. All the adatoms are in the epitaxial positions and all the original surface dimers are open. We note that some correlated motion mechanisms were observed in the overlayer structures also, and they too were terminated only when they encountered an amorphous region. Recent experiments that examine MBE growth on Si{100} using STM (16,17) have observed surface structures that are indicative of our mechanism of anisotropic growth.

Lastly in this section, we note that the models of microscopic reaction mechanisms for the unreconstruction of the original reconstructed surface and the formation of epitaxial layers in the deposited material have been used successfully to grow a few monolayer thick Si and Ge epitaxial films on Si{100}-(2x1) surface (13,14). The macroscopic growth modes extracted from these studies are described

elsewhere (14).

### *IV. The dynamics of F atom reaction with Si(100)-(2x1) surface; sticking probability as a function of coverage*

The sticking probability of 0.039 eV F atoms on a Si{100}-(2x1) surface as a function of coverage, $\theta$, is studied for five different coverages: $\theta$=0, 1/8, 1/2, 7/8 and 1. The resulting adsorption curve is shown in Fig. 5. The circles are the calculated data points and the solid line is the Langmuir adsorption curve, $S(\theta)=S_o(1-\theta)$, where the sticking probability on the clean surface ($S_o$) is 0.95. There are three interesting observations that result from this study. First, the sticking probability of F atoms on the clean surface is not unity. Even though the surfaces possesses a high density of adsorption sites, i.e. one dangling bond per surface atom, 5% of the F atoms do not adsorb to the surface. The aiming points of all the F atom trajectories which do not stick are over the third layer atoms. Second, for $\theta$ = 1/8 and 7/8, diffusion does not appear to play a role in determining the adsorption probability of the fluorine atom. The fluorine atoms in these cases adsorb only if they are aimed directly over a dangling bond site. Third, for some of the assumed ordered overlayers of the $\theta$=1/2 coverages, the sticking probability does not follow the Langmuir adsorption curve. Fig. 6(a-d) shows four assumed ordered overlayers for $\theta$=1/2. The sticking probabilities for these surfaces are 0.47, 0.51, 0.61, and 0.62, respectively. The two values larger than that predicted by the Langmuir isotherm, i.e. the surfaces in Fig. 6(c) and 6(d), warrant special attention as it appears that surface diffusion may now be important.

In order to obtain an approximate dynamical representation of fluorine reactivity to these surfaces in a static contour plot, we have calculated minimized energy contour plots as shown in Figs. 7(a-d) for the surfaces in Figs. 6(a-d), respectively. In each case the square region represents the entire crystal as shown in Fig. 6. The goal is to identify the regions of the surface which are attractive to an incoming fluorine atom. A grid of 21 x 21 points is used in making the contour plots. At each point, a fluorine atom is placed above the surface outside the influence of the potential energy function with a kinetic energy of $4.6 \times 10^{-4}$ eV directed towards the surface. The incident fluorine atom's lateral positions are fixed. The system minimizes its energy by changing the coordinates of the atoms in the substrate and the perpendicular coordinate of the incident fluorine atom. The energy minimum is found by integrating the equations of motion for the combined system for 2,000 timesteps at 300 K and then zeroing the velocities for an additional 2,000 timesteps. The adsorption energy is obtained by subtracting the energy of the initial crystal from the energy value found by the above procedure. The energies resulting from the minimization indicate that an aiming point is either attractive (having an energy difference between -2.25 and -5.59 eV) or not attractive (having and energy difference between 0.00 and -0.13 eV). Therefore, we feel that this type of contour plot gives a reasonable qualitative representation of the dynamical reactivity of an incident fluorine atom with the surface. We have plotted energy contours between -2.5 and -5.3 eV in steps of 0.4eV. The attractive regions of the surface are those that have the highest density of lines.

The difference between the sticking probability values for Fig. 6(c-d) and 6(a-b) can be accounted for by comparing the size of the attractive areas in the energy contours in Fig. 7. The total area of attraction appears larger in Fig. 7 (c-d) than in Fig. 7 (a-b). The attractive areas over the dangling bond sites are discreet in Fig. 7(b) and nearly discreet in Fig. 7 (a) whereas the attractive areas over the dangling bond sites in Fig. 7(c-d) are connected by attractive trough which are either parallel or perpendicular to the dimer rows. We conclude that the chain-like fluorine overlayers in Fig. 6(c-d) permit the formation of attractive bridges between dangling bond sites. These bridges therefore increase the sticking probability value since a fluorine atom which is aimed at these positions will feel some attraction and can therefore be pulled towards a dangling bond. Fig. 7(a) also has troughs of attraction between the dangling bond sites, however, these trough are much narrower. Based upon the conclusion that attractive troughs which join dangling bond sites increase the sticking probability of a surface, the sticking probability of the overlayer in Fig. 6(a) should be larger than the overlayer in Fig. 6(b). The results of the calculations, however, give the opposite trend. Since the sticking probability values were calculated with a rather small number of trajectories, we feel that the uncertainty in the values is larger than their difference.

Engstrom, *et. al.* (6) have experimentally determined the sticking probability of atomic fluorine on the clean Si{100}(2x1) surface to be 0.5±0.3. The large uncertainty of their result was attributed to the low concentration (17%) of atomic fluorine in the beam which also contained molecular $F_2$ and a seed gas. To obtain the atomic sticking probability, the sticking probability due to pure $F_2$ had to be subtracted from the total signal. Our result of near unity for the sticking probability on the clean surface seems more logical considering the density of dangling bonds on the surface and the large exothermicity. Our simulations show that the sticking probability depends on coverage whereas experimentally the dependence is found to be weak (6). This discrepancy could be due to an unrealistic potential energy function or to the inability to obtain an experimental crystal which is totally free of contamination and defects.

## *V. Comments*

To summarize the inferences drawn from these simulations we first review the microscopic mechanisms of surface unreconstructions during the initial stages of the epitaxial growth, and then comment upon F atom adsorption to the Si surface. It is found that the openings of the dimers on Si{100}-(2x1) surface occur through two distinct mechanisms, a) the diffusing adatom induced bumping of the adatom on the dangling bond into the dimer, and b) direct insertion of the incoming adatoms into epitaxial positions. The former is the primary mechanism of unreconstruction during the equilibration process while the latter occurs mainly during the deposition process. The number of both types of such occurrences increases by increasing the temperature of the substrate. The diffusing adatom induced dimer opening [Fig. 2b] can also sometimes cause interlayer mixing across the growing interface. The growth of Si/Si{100} thin film, presented in detail elsewhere (13), revealed a novel mechanism of correlated adatom motion induced dimer openings which is more

favored in a direction perpendicular to the direction of the dimer rows on the original reconstructed surface. This mechanism may be responsible for the anisotropic nature of the epitaxially grown layers as observed in some recent STM studies (16,17). The dimer opening of the Si{100} surface due to Ge deposition was mainly through the direct insertion mechanism, however, a few correlated adatom motion induced dimer openings were also observed. Here we also note that the dimer opening reaction mechanisms as described in this work can be used successfully to explain the layer by layer formation of epitaxially grown regions.

We have calculated the dependence of the sticking probability of atomic fluorine on Si{100}(2x1) surface on coverage using near thermal fluorine atoms. We found the initial sticking probability to be near unity. Our values for the sticking probability versus coverage are close to those predicted by Langmuir adsorption for low and high coverages, thus surface diffusion does not play a dominant role. However, for some assumed geometries of a half monolayer coverage we note that diffusion leads to an enhanced sticking probability.

*Acknowledgments*

The authors graciously thank the Office of Naval Research, the National Science Foundation, the IBM Program for the Support of the Materials and Processing Sciences, and the Camille and Henry Dreyfus Foundation for financial support. The Pennsylvania State University supplied a generous grant of computer time for this work. We would like to thank F. H. Stillinger for providing a copy of reference 6 prior to publication and also for providing the $F_3$ potential parameters in silicon reduced units. Discussions with D. W. Brenner have been most helpful.

*References*


1. J. Bevk, J. P. Mannaerts, L. C. Fedman and B. A. Davidson, *Appl. Phys. Lett.* **49**, 286 (1986).
2. I. Ihm, M. L. Cohen, and D. J. Chadi, *Phys. Rev.* **B21**, 4592 (1980).
3. R. M. Tromp, R. J. Hamers, and J. E. Demuth, *Phys. Rev. Lett.* **55**, 1303 (1985).
4. R. J. Hamers, R. M. Tromp and J. E. Demuth, *Phys. Rev.* **B34**, 5343 (1986); *Surf. Sci.* **181**, 346 (1987).
5. For a recent review, see: D. Haneman, *Rep. Prog. Phys.* **50**, 1045 (1987).
6. J. R. Engstrom, M. M. Nelson and T. Engel, *Surf. Sci.* **215**, 437 (1989).
7. C. D. Stinespring and A. Freedman, *Appl. Phys. Lett.* **48**, 718 (1986).
8. F. R. McFeely, J. F. Morar, and F. J. Himpsel, *Surf. Sci.* **165**, 277 (1986).
9. F. H. Stillinger and T. A. Weber, *J. Chem. Phys.* **88**, 5123 (1988).
10. F. H. Stillinger and T. A. Weber, *Phys. Rev. Lett.* **62**, 2144 (1989).
11. J. Tersoff, *Phys. Rev.* **B39**, 5566 (1989).
12. F. H. Stillinger and T. A. Weber, *Phys. Rev.* **B31**, 5262 (1985).
13. D. Srivastava, B. J. Garrison and D. W. Brenner, *Phys. Rev. Lett.* **63**, 302 (1989).
14. D. Srivastava and B. J. Garrison, *J. Vac. Sci. Technol. A*, to appear (1990).
15. T. A. Schoolcraft and B. J. Garrison, *J. Vac. Sci. Technol. A*, to appear (1990).
16. R. J. Hamers, U. K. Kohler and J. E. Demuth, *Ultramicroscopy* **31**, 10 (1989).
17. M. G. Lagally, R. Kariotis, B. S. Swartzentruber and Y.-W. Mo, *Ultramicroscopy* **31**, 87 (1989).
18. H.-J. Gossmann and L. C. Feldman, *Phys. Rev.* **B32**, 6 (1985).
19. H. J. C. Berendsen, J. P. M. Postma, W. F. Gunsteren, A. Dinola, and J. R. Hoak, *J. Chem. Phys.* **81**, 3684 (1984).
20. R. Biswas, G. S. Grest and C. M. Soukoulis, *Phys. Rev.* **B38**, 8154 (1988).
21. D. W. Brenner and B. J. Garrison, *MRS Symposia Proceedings* **94**, 77 (1987); *Surf. Sci.* **198**, 151 (1988).
22. D. W. Brenner and B. J. Garrison, *Phys. Rev.* **B34**, 1304 (1986).
23. M. J. Bozack, M. J. Dresser, W. J. Choyke, P. A. Taylor and J. T. Yates, Jr., *Surf. Sci.* **184**, L332 (1987).

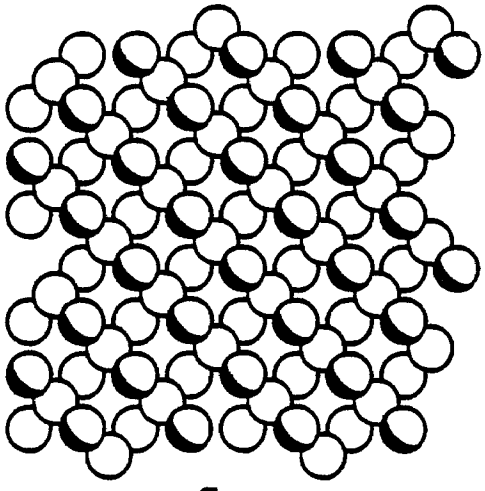


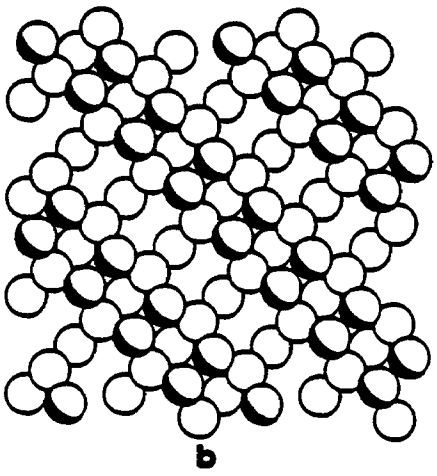


Fig. 1. Top views of (a) the bulk terminated, and (b) (2x1) dimer reconstructed Si{100} surface. On the reconstructed surface in (b), surface atoms have moved closer to the neighboring atoms and have formed rows of stable (2x1)-dimer reconstructions.

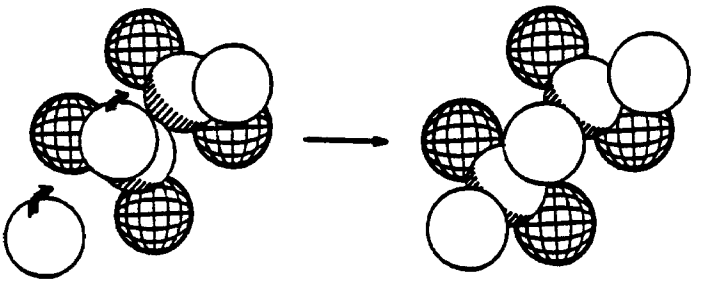

a

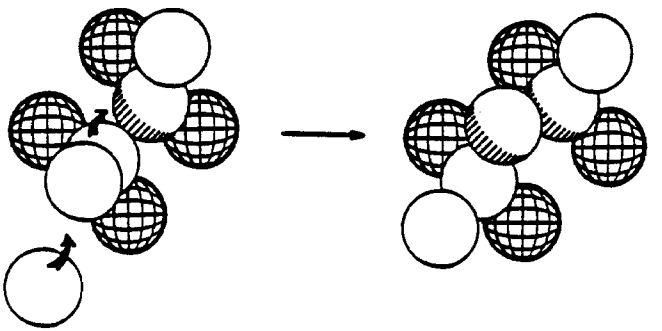

b

Fig. 2. Diffusing adatom motion induced mechanisms of dimer openings. Only a subset of atoms are shown. a) The inner layer surface Si atoms are hatched and the surface dimer Si atoms are shaded. The curly arrows indicate roughly the positions to which adatoms and dimer atoms move during 0.5-1.0 ns of equilibration. Atoms of open surface dimers and epitaxially placed adatoms are shown as the final products. b) Same as (a) except that the mechanism is that of the formation of a defect.

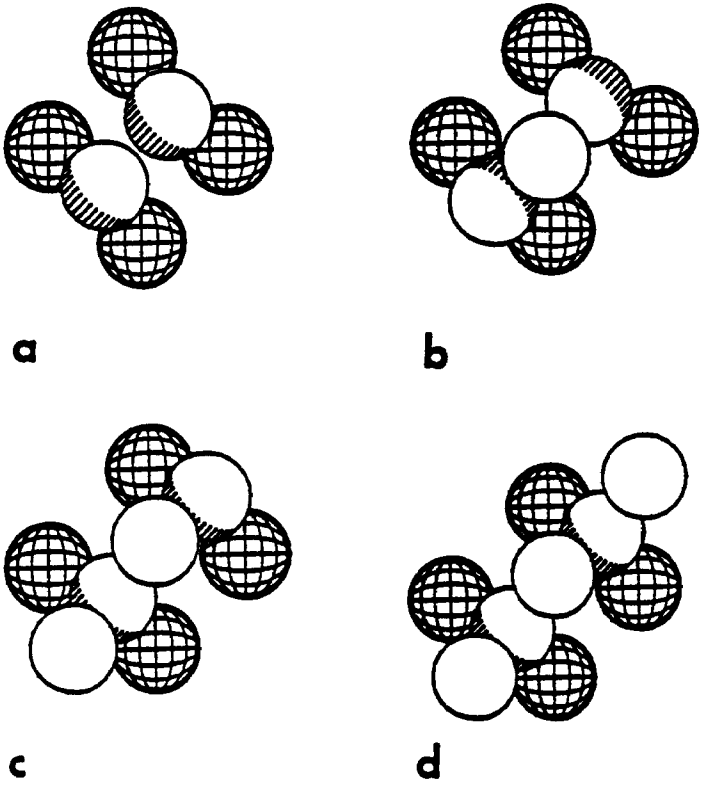


Fig. 3. a) Inner layer Si atoms (hatched) and a bare dimer (shaded). b) Direct insertion of the incoming adatom into the epitaxial position, c) and d) are same as b) except that either one or both of the dangling bonds are occupied.

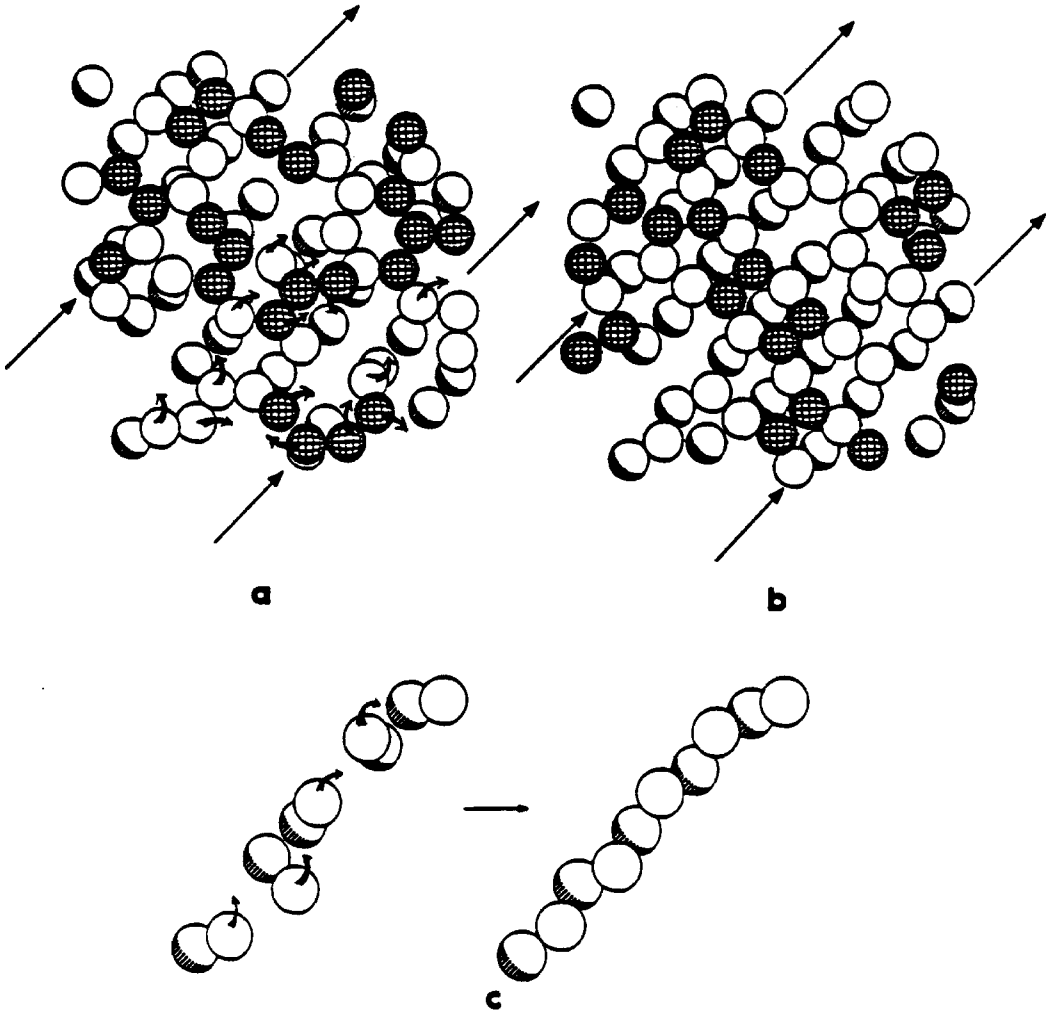


Fig. 4. Anisotropic dimer opening mechanism. a) The original reconstructed surface of Figure 1(b) after the deposition of 1.5 ML Si atoms at 800K. The curly arrows indicate the directions the adatoms move in the next 0.512 ns. The straight arrows on the side of the crystal are a guide to the periodic boundary conditions and the correlated adatom motion mechanism (see text). b) The surface and 1.5 ML Si adatoms after about 0.512 ns equilibration at 800K. c) Anisotropic dimer opening mechanism, which started in the lower left corner of (a), in isolation.

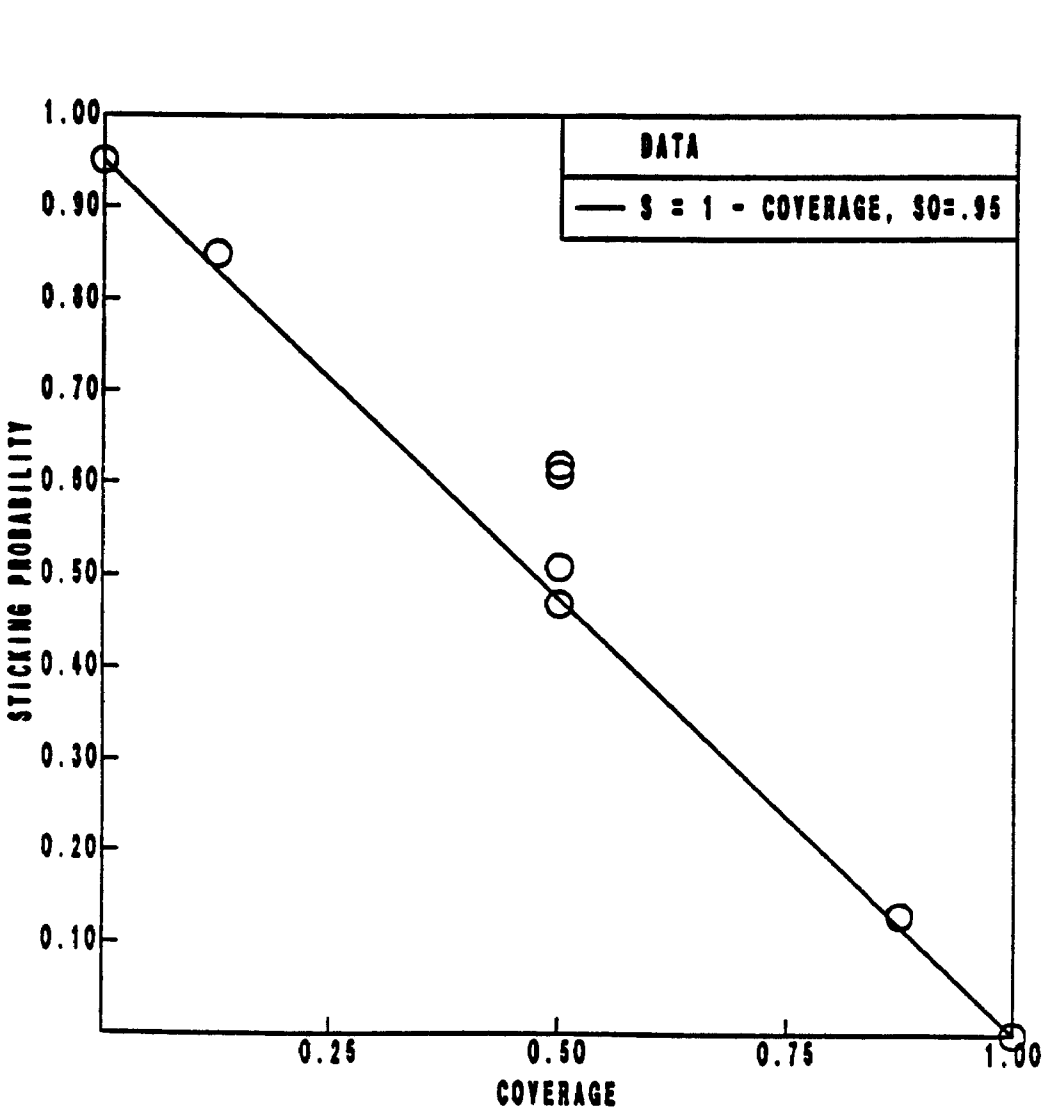


Fig. 5. The sticking probability of F atoms on Si{100} (2x1) versus F coverage. The circles are the data points calculated by the simulations. The solid line is the Langmuir adsorption curve $S(\theta)=S_0(1-\theta)$, where $S_0=0.95$.

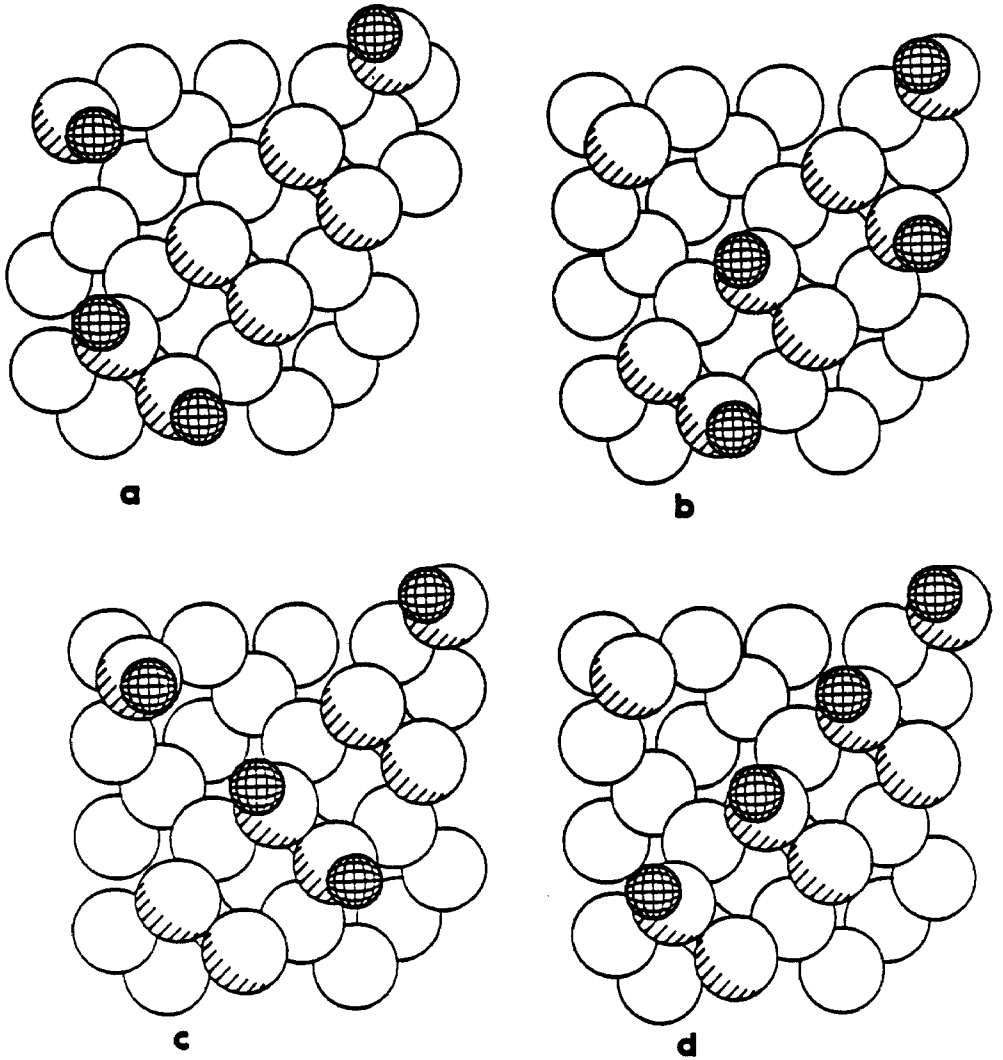


Fig. 6. One-half monolayer fluorine coverges on the Si{100}(2x1) surface. The shaded atoms are the surface dimers and the open circles are the lower layers of silicon. The hatched atoms are the fluorine atoms adsorbed to the silicon dangling bonds. The periodic boundary conditions are along the surface plane.

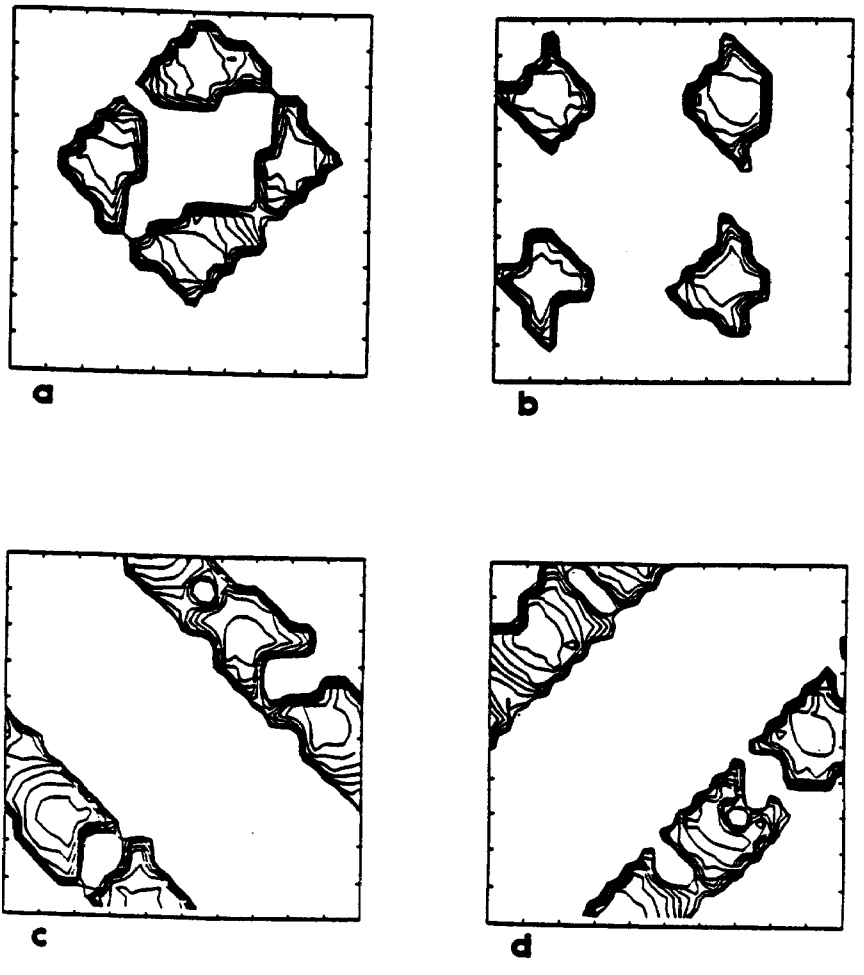


Fig. 7. Minimized energy contour plots with respect to an incident fluorine atom for the $\theta$=1/2 surfaces in Fig. 6. Constant energy contour lines are from -2.5 to -5.3 eV in steps of 0.4 eV.